Supporting Information

Bousette et al. 10.1073/pnas.1013555107

SI Methods

Echocardiographic Analysis. To measure cardiac function, mice were lightly anesthetized with isoflurane gas (1.5%) and transthoracic measurements were taken using Sequoia (Aquson) with a 13-MHz linear probe array. Two-dimensional M-mode images were acquired using a high-resolution zoom with a sweep speed of 200 mm/s from the short axis view at the papillary muscle level. Five independent measurements of left ventricular (LV) anterior wall thickness, posterior wall thickness, LV end-diastolic dimension (EDD), and LV end-systolic dimension (ESD) were taken from each of four different M-mode images for a total of 20 measurements for each mouse for each parameter. These values were then averaged for each mouse. Fractional shortening percentage was calculated from the standard equation (EDD – ESD)/EDD ×100%. Body temperature was maintained by a heating pad.

Sample Preparation. Calcineurin A (CNA) mice and their WT littermates were killed by CO_2 asphyxiation at 14 and 24 wk. Hearts were harvested and ventricular tissue was isolated and rinsed thoroughly with ice-cold PBS to remove any remaining blood. Tissue was pooled from six mice and placed in an ice-cold lysis buffer [250 mM Sucrose, 50 mM Tris-HCl (pH 7.4), 5 mM $MgCl_2$, 1 mM DTT, 1 mM PMSF]. Tissue was dounce-homogenized and differential centrifugation was carried out to isolate cytosolic, microsomal, and mitochondrial fractions. Specifically, we separated contractile proteins and nuclei from cytosolic, microsomal, and mitochondrial proteins by centrifuging the cardiac lysate for 15 min at 4 °C at 800 × *g*. This supernatant contains the majority of cytosolic, microsomal [i.e., endoplasmic reticulum (ER), golgi, vesicles, plasma membrane), and mitochondrial fractions. Using this fraction we next separated out the cytosolic and microsomal proteins from mitochondrial proteins by centrifuging the latter supernatant at 9,000 × *g* for 20 min at 4 °C. The resultant supernatant contains the cytosolic and microsomal proteins and the resultant pellet contains the mitochondrial proteins. The pellet is kept on ice while the cytosolic/microsomal protein separation is carried out. To separate out the cytosolic from microsomal proteins, 1.8 mL 2.5 M KCl is added to the latter supernatant, which is then centrifuged for 60 min at 180,000 × *g* (33,000 rpm) at 4 °C. The resultant supernatant contains the cytosolic proteins and the resultant pellet contains the microsomal proteins. Next, we resuspended the latter pellet in 500 μL Lysis buffer + 1.5% Triton-X to solubilize the microsomal proteins. Next, to separate mitochondrial matrix proteins from mitochondrial membrane proteins, we resuspended the mitochondrial pellet in 1 mL 10 mM hepes. We sonicated the suspension (20 pulses on a low-medium setting) and then incubated the suspension for 30 min on ice. After incubation, the suspension was centrifuged for 30 min at 4 °C at 16,900 × *g*. The resultant supernatant contains the mitochondrial matrix proteins and the resultant pellet contains the mitochondrial membrane proteins. We resuspended the pellets in 0.5 mL Lysis buffer + 1.5% Triton-X to solubilize mitochondrial membrane proteins.

Proteomics Analysis. Aliquots containing 100 μg of total protein from each fraction were precipitated with ice-cold acetone, reduced, alkylated, and digested sequentially with endoproteinase Lys-C and trypsin overnight, as described previously (1, 2). These peptides were solid-phase extracted and acidified by the addition of formic acid. Samples were loaded onto separate microcapillary fused silica columns (internal diameter of 100 μm) containing strong cation exchange resin (Parisphere; Whatman) and reverse-phase resin (Zorbax Eclipse XDB-$C1_8$; Agilent Technologies). Peptides were eluted from the columns by way of a 12-step × 100 min salt/water acetonitrile gradient (3). An LTQ linear ion trap mass spectrometer was placed in alignment with the columns and eluted peptides were analyzed via electrospray ionization (Thermo Fisher). A total of 4,893,830 spectra were acquired and searched against a nonredundant sequence database populated with 69,614 mouse proteins obtained from EBI Integr8 (UniProt Knowledgebase Release 15.9, Oct. 2009), using the SEQUEST search algorithm [SEQUEST-PVM v.27 (rev. 9) (1993)]. To determine the empirical false-discovery rate, spectra were searched against protein sequences in both the normal (Forward) and inverted (Reverse) amino acid orientations. The STATQUEST filtering algorithm was then applied to all match results to obtain a measure of the statistical reliability (confidence score) for each candidate identification. A cutoff *P* value of 0.01 was set, corresponding to a 99% or greater likelihood of being a correct match (2, 4).

Normalization and Filtering Procedures. All high-confidence spectra for each protein were summed across subcellular fractions for CNA mice and their WT littermates to determine relative protein abundance. Differences in protein expression between CNA and WT hearts recorded between the 64 experimental runs may demonstrate biologically relevant differences in protein expression but may also represent bias and noise. To minimize this, normalization was performed with a global scaling parameter on spectral counts derived from raw data, as previously described (1). First, data from all experimental runs was segregated into 100 bins on the basis of raw, spectral count value distribution. Bins were normalized using the LOWES S algorithm, which calibrates the data by using a globally weighted polynomial regression (5). This global normalization parameter provided a smoothed version of the spectral data and accounted for variances that occur in different experimental runs, thus providing a more accurate view of protein expression.

Upon normalization of proteomics data, a statistical test was carried out to evaluate the dependency of CNA overexpression on alteration in protein abundance, as described previously (1). Two linear models were constructed, with the first model including control and disease states (CNA and WT mice), time (14 and 24 wk), and subcellular localization (cytosol, microsomes, mitochondrial matrix, and mitochondrial membrane) as independent parameters. The second model only considered time (14 and 24 wk) and subcellular localization (cytosol, microsomes, mitochondrial matrix, and mitochondrial membrane) as independent parameters. A null hypothesis was formed, which stated that there was no observable difference between these two models (6). Significantly altered protein abundance was represented by a P value < 0.05, thereby demonstrating dependency on the disease state.

ImmunoBlot Analysis. Total cellular protein was harvested from cardiac ventricular homogenates from 14-wk-old CNA and WT animals and was subjected to standard Western blotting techniques (1). Protein concentrations were determined using Bradford assay and equal protein loading conditions were verified using Ponceau staining of the membrane. Commercial antibodies were used to target specific proteins: rabbit polyclonal to four and a half LIM domain (FHL1) (Imagenex/Cedarlane Laboratories), mouse monoclonal to moesin (Santa Cruz Biotechnology, SCB), goat polyclonal to transferrin (SCB), mouse monoclonal to major vault protein(SCB), rabbit polyclonal to glucose phosphate isomerase (SCB), rabbit polyclonal to sarcolemmal membrane associated

protein (a kind gift from Balwant Tuana, Faculty of Medicine, University of Ottawa, Ottawa, ON, Canada), rabbit polyclonal to Bag3 (Alexis Biochemicals), mouse monoclonal to Hsp70 (Affinity Bioreagants), mouse monoclonal to cardiac myosin heavy chain (Affinity Bioreagents), rabbit polyclonal to destrin (Abcam), mouse monoclonal to atrial natriuretic factor (Abcam), mouse monoclonal to annexin 2 (BD Biosciences), rat monoclonal to IGFBP-7 (R&D Systems), polyclonal Anti-GRP78 (Stressgen), and polyclonal Anti-PDI (Stressgen).

Histological Analysis. Whole hearts harvested at 14 wk from CNA and WT mice were washed with ice-cold PBS and then fixed with formalin. Cardiac sections were cut at a thickness of 5 μM for histological analysis. Staining of myocardium was done using either H&E or Masson's Trichrome reagents.

Microarray Analysis. Total cellular RNA was harvested from cardiac ventricular tissue samples using TRIzol, which was then reverse transcribed to cDNA using a commercially available kit (Qiagen). Microarray-based global mRNA profiling experiments were performed using the affymetrix mouse 430 2.0 full genome array chips at the University Health Network Array Facility (Toronto, ON, Canada) (1). FlexArray software was used for microarray data analysis (7). Affymetrix probes were cross-mapped to gene names for correlation analyses. Redundant accessions were averaged.

Gene Ontology Analysis. Gene ontology term enrichment analysis was carried out using an in-house, statistically based, Gene Ontology enrichment analysis tool, MouseSpec, which is publically available at http://webprod1.ccbr.utoronto.ca/mousespec/.

Lentivector Production and Transduction of Neonatal Cardiomyocytes. Second generation lentivector compatible clones expressing shRNA targeting mouse Crystallin were obtained from OpenBiosystems. The negative control scrambled shRNA construct was a kind gift from Stephane Angers (University of Toronto, Toronto, ON, Canada). Clones were amplified using the ampicilin resistance marker in DH5-α cells. Plasmids were then isolated using Qiagen maxi preps according to the manufacturer's instructions. The packaging plasmid (pCMV-R8.74psPAX2, 2.5 μg), envelope plasmid (VSV-G/pMD2.G, 0.3 μg), and the target construct plasmid (pLKO.1, 2.7 μg) expressing either the shRNA or scrambled shRNA (as a negative control) were simultaneously transfected into HEK-293T cells with Optimem (Invitrogen) diluted FuGene (Roche). Neonatal cardiomyocytes were incubated with supernatant from transfected HEK-293T cells for 21 h after which the medium was replaced daily. Because the lentivector constructs have a puromycin resistance gene, we selected for transduced cardiomyocytes by incubating with 2 μg/mL puromycin for 48 h to kill off all nontransduced cells to ensure a homogenous population of transduced cells. Transduction efficiency was >90% using a green fluorescent protein-expressing lentivector (Fig. S8).

Viability Assays. Neonatal cardiomyocytes from either CNA or WT littermates were subjected to either 72 h serum starvation or 200 μM hydrogen peroxide for 24, 48, or 72 h. Viability assays were carried out using a commercially available cell counting kit (CCK-8; Dodinjo) according to the manufacturer's instructions.

1. Gramolini AO, et al. (2008) Comparative proteomics profiling of a phospholamban mutant mouse model of dilated cardiomyopathy reveals progressive intracellular stress responses. *Mol Cell Proteomics* 7:519–533.
2. Kislinger T, et al. (2006) Global survey of organ and organelle protein expression in mouse: Combined proteomic and transcriptomic profiling. *Cell* 125:173–186.
3. Gramolini AO, Kislinger T, Liu P, MacLennan DH, Emili A (2007) Analyzing the cardiac muscle proteome by liquid chromatography-mass spectrometry-based expression proteomics. *Methods Mol Biol* 357:15–31.
4. Kislinger T, Gramolini AO, MacLennan DH, Emili A (2005) Multidimensional protein identification technology (MudPIT): Technical overview of a profiling method optimized for the comprehensive proteomic investigation of normal and diseased heart tissue. *J Am Soc Mass Spectrom* 16:1207–1220.
5. Saama PM, Patel OV, Bettegowda A, Ireland JJ, Smith GW (2006) Novel algorithm for transcriptome analysis. *Physiol Genomics* 28:62–66.
6. Isserlin R, Emili A (2008) Interpretation of large-scale quantitative shotgun proteomic profiles for biomarker discovery. *Curr Opin Mol Ther* 10:231–242.
7. FlexArray (2007) *A Statistical Data Analysis Software for Gene Expression Microarrays.* Version 1.2.

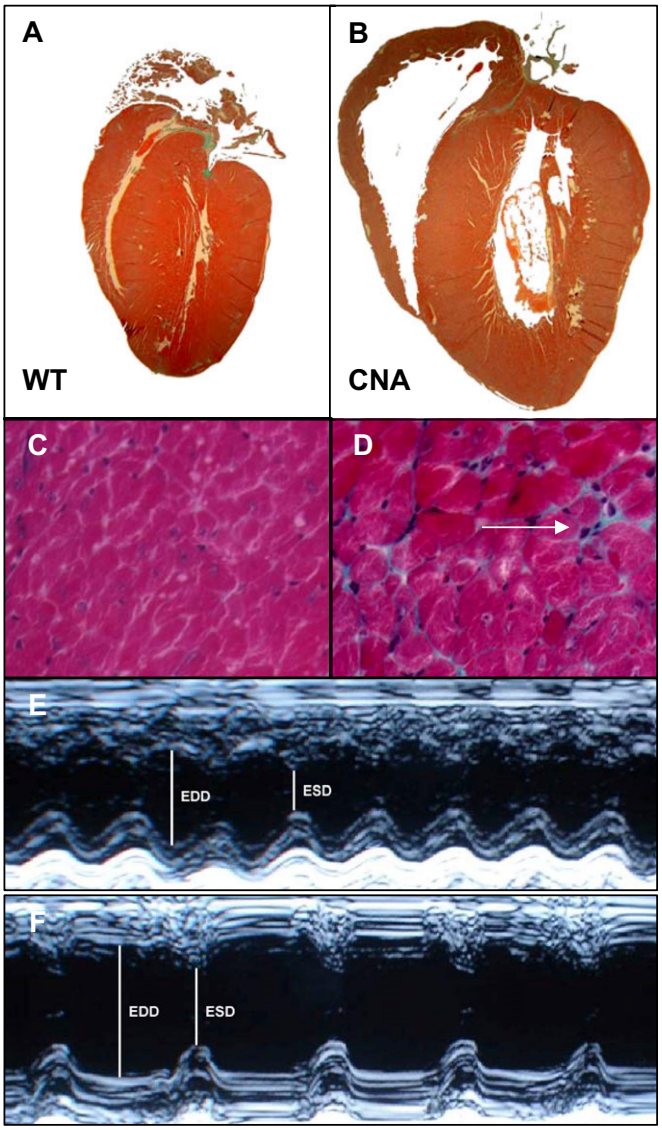

Fig. S1. Cardiac hypertrophy in CNA transgenic mice. Sagittal sections of a WT mouse heart (*A*); and a CNA mouse heart (*B*). (*C*) Masson's Trichrome stained myocardium from a WT heart and (*D*) a CNA heart demonstrating interstitial fibrosis (arrow). (*E*) A representative image of an M-mode echocardiogram of a WT mouse and (*F*) a CNA mouse. End-diastolic dimension (EDD) and end-systolic dimension (ESD).

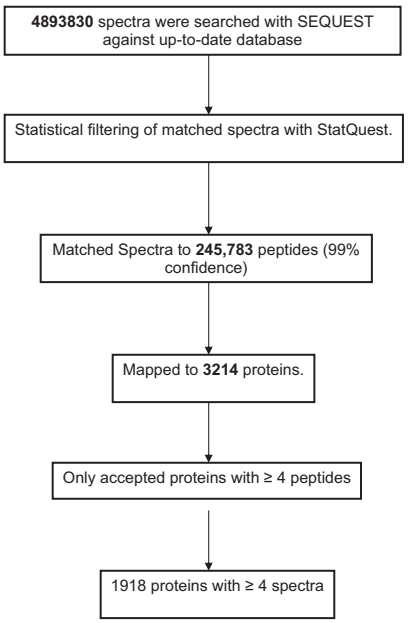

Fig. S2. A flowchart demonstrating the data flow from all spectra obtained from the liquid chromatography-mass spectrometry methodology to the identification of 1,918 proteins as the final proteome.

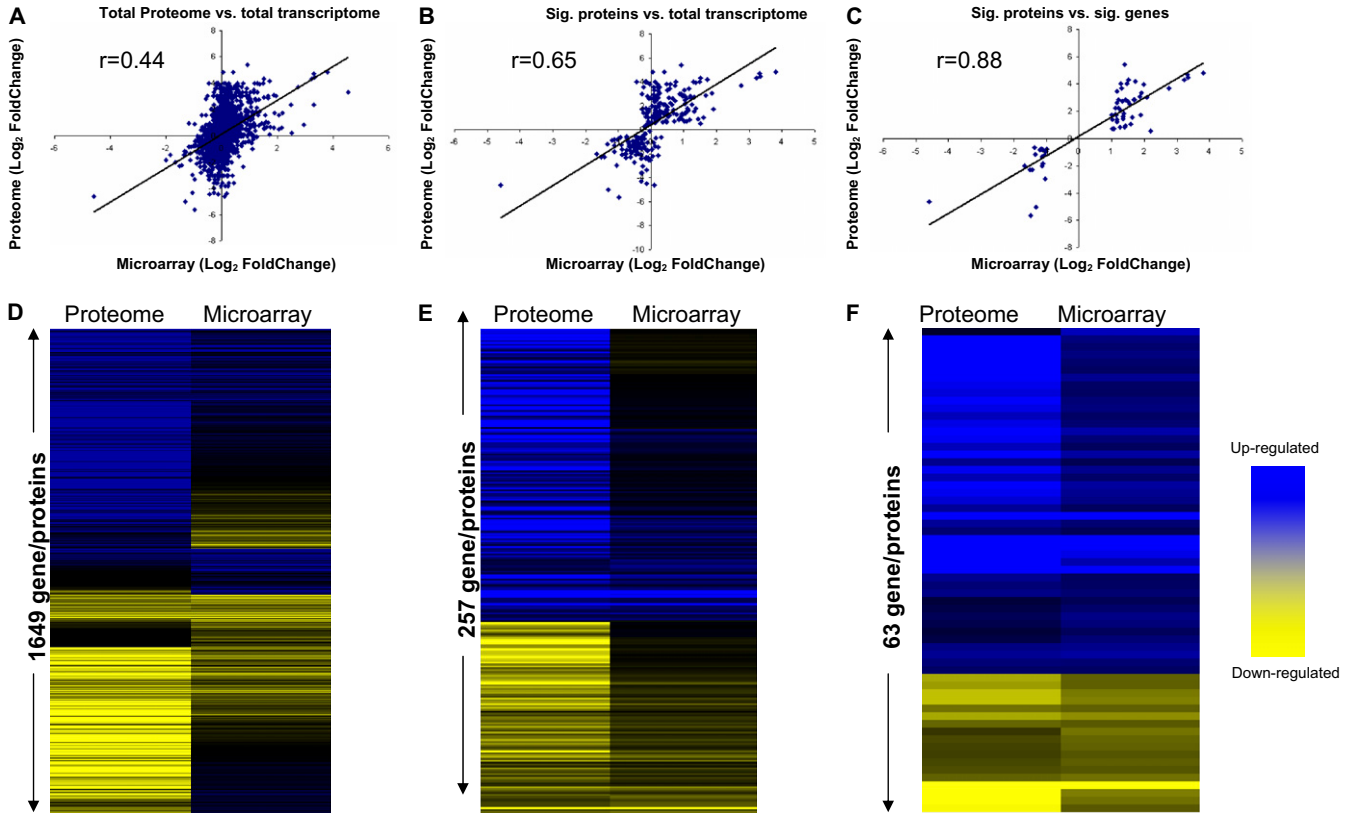

Fig. S3. Microarray/proteome comparisons. (*A* and *D*) A scatterplot and heat map, respectively, comparing the CNA/WT expression ratios of common factors of the total transcriptome vs. the total proteome. (*B* and *E*) A scatterplot and heatmap, respectively, comparing the CNA/WT expression ratios of common factors in the total transcriptome vs. the significantly altered proteins of the proteome. (*C* and *F*) A scatterplot and heatmap, respectively, comparing the CNA/WT expression ratios of common factors in the significantly altered genes of the transcriptome vs. the significantly altered proteins of the proteome. A blue color in the heat maps represents up-regulated proteins/transcripts and yellow indicates down-regulated proteins/transcripts.

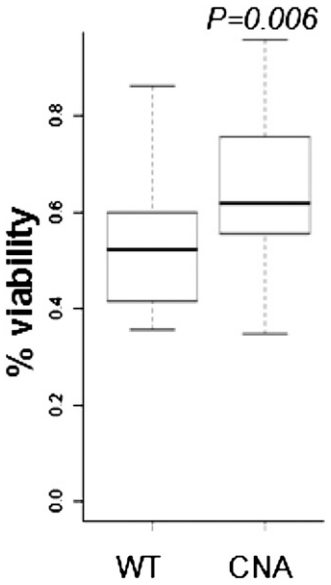

Fig. S4. Boxplot demonstrating significantly increased viability of CNA neonatal mouse cardiomyocytes (NCMs) following 72 h of serum starvation, compared with WT NCMs.

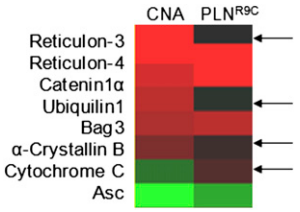

Fig. S5. List of eight potential apoptotic regulators and a heatmap demonstrating the fold-expression of these proteins in the "significantly altered proteins" subset of the CNA and PLNR9C proteomes, respectively (red bars indicate up-regulated in CNA mice, green bars indicate down-regulated in CNA mice, and black bars indicate no significant change in the PLNR9C model). Arrows indicate proteins with differential expression between the two proteomes.

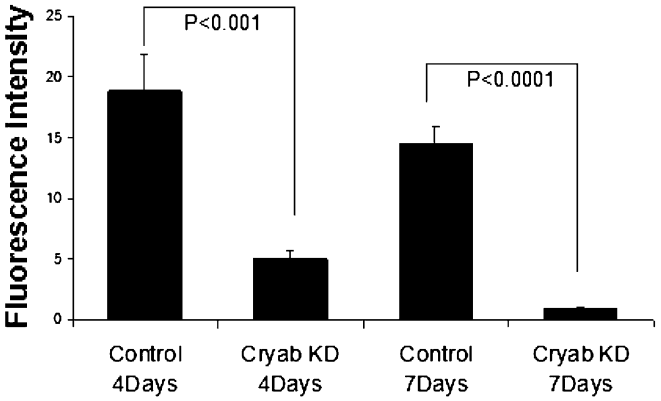

Fig. S6. Bar graph demonstrating the quantification of immunofluorescence in Fig. 4 *C–F*.

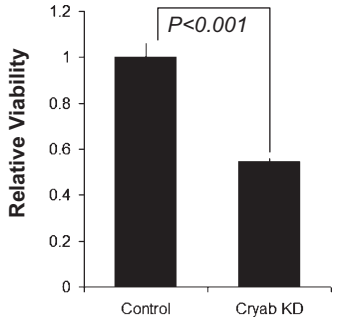

Fig. S7. Bar graph demonstrating the significant reduction in viability of WT NCMs transduced with lentivectors expressing the Cryab targeting shRNAs, compared with the WT NCMs transduced with the control lentivectors expressing the scrambled shRNAs. Both cultures were incubated with serum-free media and 200 μmol/L H_2O_2 for 48 h.

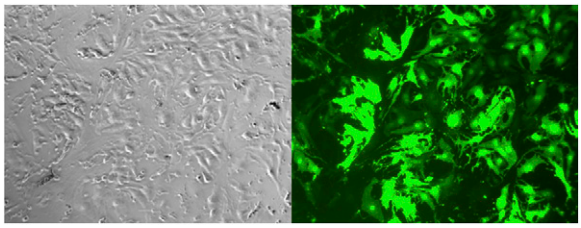

Fig. S8. Matching bright field (*Left*) and fluorescent (*Right*) photomicrographs of NCMs transduced with lentivectors expressing GFP demonstrating >90% transduction rate.

Other Supporting Information Files

Table S1 (PDF)
Table S2 (PDF)
Table S3 (PDF)
Table S4 (PDF)
Table S5 (PDF)
Table S6 (PDF)
Table S7 (PDF)
Table S8 (PDF)
Table S9 (PDF)
Table S10 (PDF)